Reprinted from Journal of the AMERICAN HELICOPTER Society, April, 1972

Linear Flap-Lag Dynamics of Hingeless Helicopter Rotor Blades in Hover

Robert A. Ormiston and Dewey H. Hodges,
Research Scientists
Ames Directorate
U. S. Army Air Mobility Research & Development Laboratory
Ames Research Center
Moffett Field, California

The linear stability characteristics of rotor blade flap-lag oscillations in the hovering flight condition are examined. The present study is focused on the effects of pre-cone, variable elastic coupling, pitch-lag coupling, and the aerodynamics of induced inflow. Together with an improved perturbation analysis for deriving the equations these factors are shown to significantly influence the flap-lag stability characteristics of hingeless rotor blades. Routh's criteria are used to derive several fundamental flap-lag stability relations, and emphasize the utility of simplified rotor blade modeling for understanding complex dynamic phenomena. In order to validate the approximate rigid blade equations, elastic blade modal equations are presented together with comparative solutions. The results indicate a high degree of accuracy for the approximate equations when the elastic coupling is included. Finally, the approximate equations are used to illustrate the influence of elastic coupling on the response characteristics of hingeless rotors.

NOMENCLATURE

a	= two-dimensional lift curve slope
A, A_{approx}, C	= induced flow parameters, Eqs. (7, 41).
b	= number of blades
c	= blade chord, ft
c_{d_0}	= profile drag coefficient
$C_\beta, C_{\dot\beta}, C_\zeta, C_{\dot\zeta}$	= lead moment coefficients
dD, dL, dF_z, dF_y	= local lift and drag forces; flap and lead components, lb/ft
E	= Young's modulus, lb/in^2
F	= Routh's discriminant, Eq. (9)
$F_\beta, F_{\dot\beta}, F_\zeta, F_{\dot\zeta}$	= flap moment coefficients
D	= drag parameter $2c_{d_0}/a$
I	= blade inertia, $^1/_3 mR^3$, slug-ft^2
I_1, I_2	= blade section principal moments of inertia
K_{β_H}, K_{ζ_H}	= flap and lead-lag spring rates at hub, ft-lb/rad, Fig. 14
K_{β_R}, K_{ζ_R}	= flap and lead-lag spring rates at blade root, ft-lb/rad, Fig. 14
K_β, K_ζ	= total flap and lead-lag hinge spring rates at $\theta = 0$, ft-lb/rad, Eq. (43)
K_{vv}, K_{vw}, K_{wv}	= elastic blade stiffness parameters, Eqs. (56–58)
m	= blade mass distribution, slug/ft
n	= number of elastic blade flap and in-plane modes
$M_{\beta aero}, M_{\zeta aero}$	= flap and lead aerodynamic moments, Eqs. (39, 40)
p, P, q	= rotating flap and lead-lag frequency parameters, Eqs. (11, 25, 27, 51)
R	= blade radius, ft; also, variable elastic coupling parameter, Eq. (47)
R_w	= elastic coupling parameter, Eq. (51)
s	= Laplace transform variable, sec^{-1}
T	= rotor blade tension, lb
u, v, w	= displacements in x, y, z direction measured from undeformed positions, ft
U_P, U_T	= relative normal and tangential airfoil velocities, fps, Eq. (34)
v_i	= induced velocity, fps
V, V_T	= velocity, velocity of blade tip. $R\Omega$, fps
V_n, W_n	= generalized coordinates for modal equations
W	= lead-lag frequency parameter, Eqs. (11, 25, 27)
x, y, z	= rotating coordinates
z, Z	= elastic coupling parameters, Eqs. (51, 25)
β	= flapping angular displacement of blade measured from plane of rotation, rad
$\beta_{pc}, \beta_{pc_\zeta}, \beta_{pc_w}$	= pre-cone parameters, Eqs. (17, 18)
γ	= Lock number, $\rho acR^4/I$
Δ	= elastic coupling parameter, Eq. (46)

ζ = inplane, or lead-lag angular displacement of blade, rad
η = Lock number parameter, $\gamma/8$
η_m = structural damping parameter
θ = blade pitch angle, rad
$\theta_{\min}$ = minimum θ for neutral stability for given p
θ^* = absolute minimum θ for neutral stability
θ_ζ = kinematic pitch-lag coupling parameter
ξ = nondimensional radial coordinate, x/R
ρ = air density, slugs/ft^3
σ = rotor solidity, $bc/\pi R$
σ_ζ = real part of inplane mode eigenvalue, sec^{-1}
ϕ, ϕ_t = inflow angle, $\phi = \tan^{-1} U_P/U_T$, $\phi_t = v_t/\Omega x$
ϕ_{v_n}, ϕ_{w_n} = mode shapes for modal equations
Ω = coordinate system angular velocity, rad/sec
ω = imaginary part of eigenvalue, rad/sec
$\omega_\beta, \omega_\zeta$ = flap and lead-lag non-rotating frequency, Eq. (51), rad/sec
$(\dot{})$ = $d(\ )/dt$
$(\ )'$ = $\partial(\ )/\partial x$
$(\ )_0, \Delta(\ )$ = steady state and perturbation variables
$(\bar{})$ = nondimensionalized by R for lengths, V_T for velocities Ω for frequencies.

THE GROWING acceptance of hingeless rotors for conventional and compound helicopters has intensified the need for fundamental research on rotor blade stability. This is because the small aerodynamic and structural damping of the lead-lag motion can lead to unstable rotor blade oscillations. The lack of a lead-lag hinge and the desire for simplicity usually preclude the use of auxilliary viscous dampers which are normally used to augment damping of articulated rotor blades.

The fundamental stability characteristics of hingeless rotor blades can be studied by retaining only the flap and lead-lag degrees of freedom of a single blade. Several researchers have already studied this problem,[1-5] however, the subject of flap-lag stability is not yet adequately understood. In particular, the effects of aerodynamics, pre-cone, elastic coupling, and kinematic pitch-lag coupling were either not included, incorrectly derived, or not systematically investigated. In addition, in nearly all cases only simplified mechanical representations of fully elastic hingeless rotor blades such as centrally hinged rigid blades with spring restraint were employed.

The present study was therefore undertaken to address these factors in detail. In order to determine the accuracy of the approximate equations for centrally hinged, rigid blades used by previous investigators, the exact multimode elastic blade equations are also derived and results for both formulations compared. The analysis is restricted to the hover condition which greatly simplifies the problem by eliminating the periodic coefficients of the forward flight equations. Further simplification is obtained by excluding the torsional degree of freedom. Although torsional motion is important for rotor blade stability, its inclusion is beyond the scope of the present study.

BASIC FLAP-LAG EQUATIONS

The approximate perturbation equations derived in the Appendix for the centrally hinged rigid blade with spring restraint, may be used to examine the source of potentially destabilizing flap-lag coupling. The homogeneous equations for the basic configuration (without pre-cone or elastic coupling) can be written,

$$\begin{bmatrix} s^2 + F_{\dot\beta} s + F_\beta & -sF_\zeta \\ -sC_{\dot\beta} & s^2 + C_\zeta s + C_\zeta \end{bmatrix} \begin{Bmatrix} \Delta\beta \\ \Delta\zeta \end{Bmatrix} = 0 \quad (1)$$

The coupling coefficients of interest are obtained from Eq. (50)

$$F_\zeta = \gamma/8(2\theta - A) - 2\beta_0 \quad (2)$$

$$C_{\dot\beta} = 2\beta_0 - \gamma/8(\theta - 2A) \quad (3)$$

where the coning

$$\beta_0 = [\gamma/8](\theta - A)/p^2, \quad p^2 = \bar{\omega}_\beta^2 + 1 \quad (4)$$

The first coefficient, F_ζ, combines the aerodynamic flap moment due to lead velocity with the opposing centrifugal flap moment due to centrifugal forces, $2\beta_0$. The second coefficient, $C_{\dot\beta}$, consists of a Coriolis lead moment due to flapping velocity opposed by a small aerodynamic moment. The product, $F_\zeta C_{\dot\beta}$ represents the potentially destabilizing flap-lag coupling. Approximating the induced inflow parameter A by $\theta/2$ (see below) yields the following simplified expression

$$F_\zeta C_{\dot\beta} = [(\gamma/8)\theta]^2[3/2 - 1/p^2]/p^2 \quad (5)$$

The destabilizing portion ($3/2$) is caused by the product of aerodynamic and Coriolis moments while the product of centrifugal and Coriolis moments ($1/p^2$) is stabilizing. Furthermore, the flap-lag coupling is proportional to θ^2 and is a maximum when $p = \sqrt{4/3}$. This flapping frequency is typical of present hingeless rotor helicopters. It may also be observed that flap-lag coupling exists for articulated rotors ($p = 1$, for zero flap hinge offset).

The induced inflow parameter A is defined in the Appendix, Eq. (41). The simple and useful approximation used above assumes that the induced inflow angle ϕ_t is given by one-half the blade pitch angle. Eq. (41) then

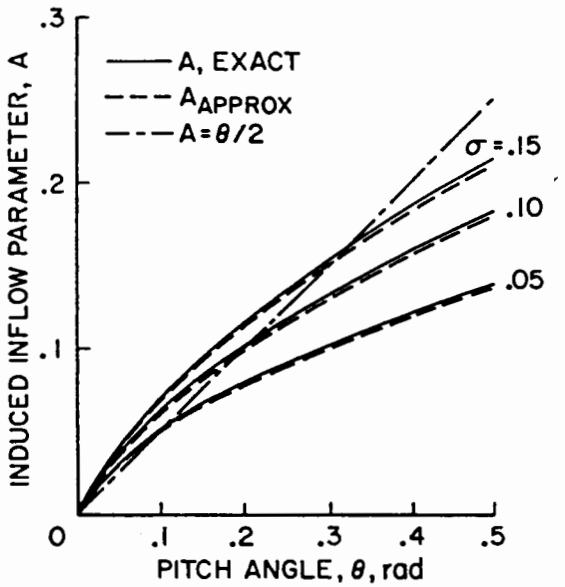

FIGURE 1. Comparison of approximations for induced inflow-parameter A.

yields $A = \theta/2$. This approximation eliminates the small aerodynamic lead moment in the lead-lag coupling coefficient $C_{\dot{\beta}}$.

Another useful but more accurate approximation for the induced inflow parameter can be derived as follows. The exact expression for A is based on nonuniform induced inflow given by blade-element momentum theory.[6] For $a = 2\pi$

$$v_i = \pi\sigma\Omega R/8[\sqrt{1 + 16\theta\xi/\pi\sigma} - 1] \qquad (6)$$

If ϕ_t is approximated by the value at $\xi = {}^3/_4$, the following equation for A results

$$A_{approx} = \pi\sigma/6[\sqrt{1 + 12\theta/\pi\sigma} - 1] \qquad (7)$$

The accuracy of these two approximate expressions is compared with the exact value in Fig. 1. The effect of solidity is seen to be important and therefore limits the usefulness of $A = \theta/2$ for quantitative results. A_{approx}, however, is quite accurate and will be used for the results which follow.

A detailed examination of flap-lag stability and dynamics will now be carried out for several specific cases. For the approximate rigid blade equations these include: 1) basic flap-lag coupling, 2) the effects of precone, 3) variable elastic coupling, and 4) pitch-lag coupling. Next, the results using multimode elastic blade equations are presented and compared with previous results and finally, the effects of elastic coupling on flapping response are examined.

RIGID BLADE STABILITY

Case I, No Pre-cone or Elastic Coupling

A broad view of the basic flap-lag stability characteristics of the rigid hinged blade is afforded by Fig. 2.

The nondimensional eigenvalues of Eq. (1) above are presented in the complex plane as a function of increasing collective pitch, for several values of inplane stiffness. The flap mode is stable in all cases, but the weakly damped lead-lag mode becomes unstable for inplane frequencies near p. Some idea of the magnitude of the instability may be gained from the time to double amplitude. With $\delta_\zeta = 0.002$ at 250 rpm, $t_{double} = 13.2$ sec, which is not particularly rapid.

The neutral stability condition ($\delta_\zeta = 0$) will now be examined with the aid of Routh's criteria. The characteristic equation of the basic flap-lag equations is a quartic of the following form

$$As^4 + Bs^3 + Cs^2 + Ds + E = 0 \qquad (8)$$

Neutral stability occurs when Routh's discriminant vanishes, i.e.,

$$F = D(BC - AD) - B^2E = 0 \qquad (9)$$

After some manipulation the following expression for the collective pitch for neutral stability is obtained.

$$(\theta - A)^2 = \frac{P^2}{2(P-1)(2-P)} \times \left\{D + \frac{[D + A\theta][P - W]^2}{\eta^2[W + P(D + A\theta)][1 + D + A\theta]}\right\} \qquad (10)$$

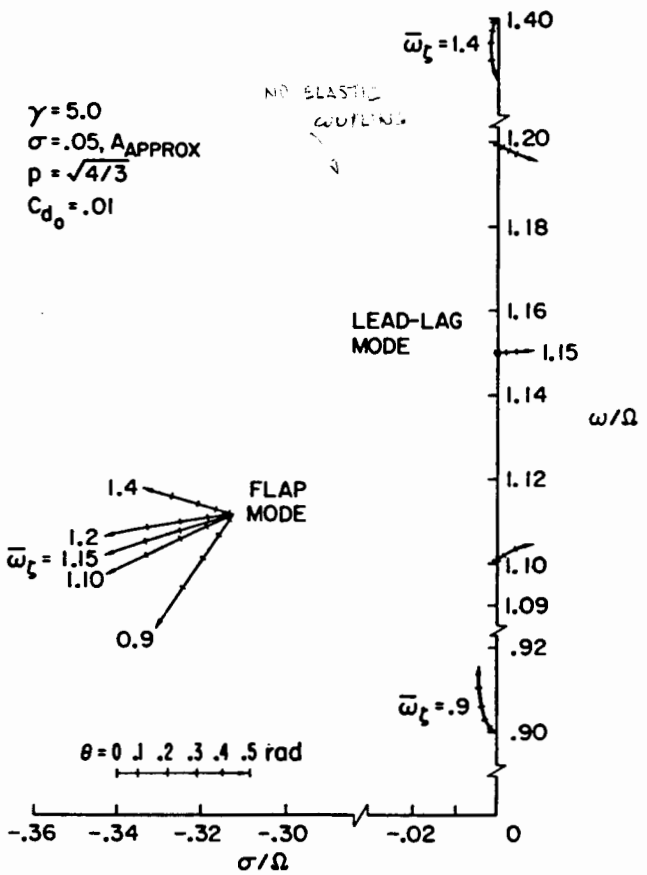

FIGURE 2. Locus of roots for increasing pitch angle, Case I, basic rigid blade equations.

where

$$D = \frac{2c_{d_0}}{a},\ P = p^2,\ W = \bar{\omega}_\zeta^2,\quad \eta = \gamma/8 \qquad (11)$$

Several conclusions immediately follow since $c_{d_0} > 0$, $A\theta > 0$. First, a necessary (but not sufficient) condition for instability is that $1 < p^2 < 2$. This indicates that purely articulated rotors without hinge offset or $\delta_3 (p = 1)$ cannot be unstable. This does not mean that destabilizing flap-lag coupling is not present, but only that it can never be sufficient to cause instability. Second, for a given flap frequency (p) the minimum pitch angle for neutral stability, θ_{min}, occurs when $\bar{\omega}_\zeta = p$ and is independent of Lock number.

$$(\theta_{min} - A)^2 = [P^2 D/2(P-1)(2-P)] \qquad (12)$$

Finally an absolute minimum can be obtained for $p = \sqrt{4/3}$. This value will be referred to as θ^* and is dependent only on the profile drag coefficient and induced inflow parameter, A. For $a = 2\pi$

$$(\theta^* - A) = 2\sqrt{c_{d_0}/\pi},\quad p = \bar{\omega}_\zeta = \sqrt{4/3} \qquad (13)$$

This simple result specifies the lowest possible pitch angle for which any hingeless rotor blade can become unstable in pure flap-lag oscillations.

Structural damping is easily incorporated by modifying the lead-lag damping coefficient C_ζ.

$$C_\zeta = \gamma/8\left[\frac{2c_{d_0}}{a} + 2\eta_m \frac{\bar{\omega}_\zeta}{\gamma/8} + A\theta\right] \qquad (14)$$

The three terms are respectively the profile drag damping, structural damping, and induced drag damping. For typical parameters $^1/_2\%$ structural damping ($\eta_m = 0.005$) is on the order of 3 times the profile drag damping which would significantly increase θ^*.

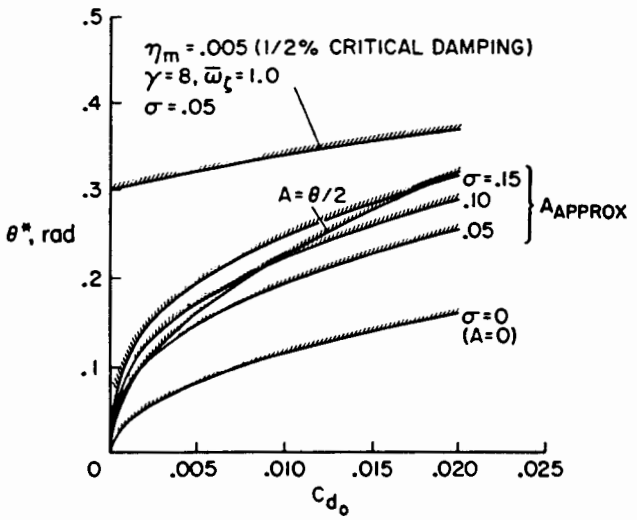

FIGURE 3. Effect of profile drag, structural damping, and aerodynamics on θ^*.

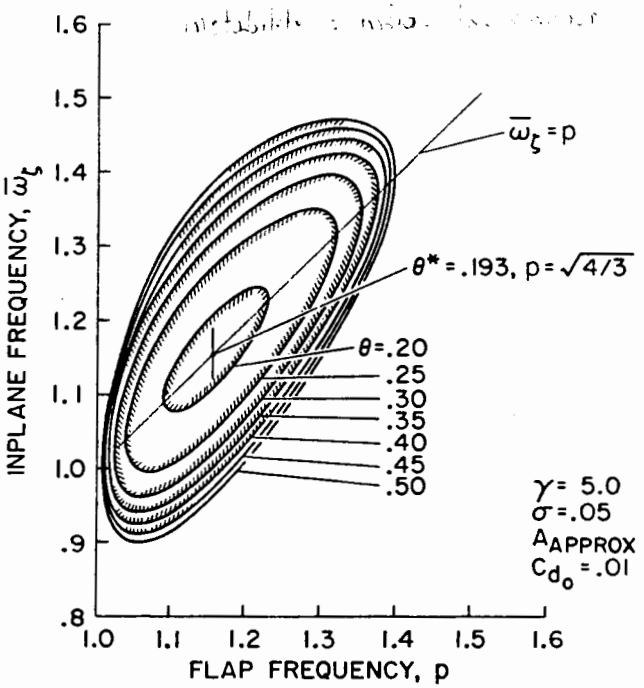

FIGURE 4. Stability boundaries for basic rigid blade equations.

Figure 3 illustrates the relationship between inplane damping and θ^* given by Eq. (13) including the effects of structural damping and various approximations for the induced inflow parameter A.

A summary plot giving basic flap-lag stability boundaries as a function of the flap and lead-lag frequencies is given in Fig. 4. For a particular collective pitch, the region of instability lies within the respective contour. These results illustrate the occurrence of θ_{min} for a given value of p when $\bar{\omega}_\zeta = p$ and θ^* when $p = \sqrt{4/3}$.

Case II, Effect of Pre-cone, No Elastic Coupling

With pre-cone, the perturbation equations are identical to those used previously although the coning now becomes

$$\beta_0 = [\gamma/8](\theta - A)/p^2 + (p^2 - 1)\beta_{pc}/p^2 \qquad (15)$$

Routh's criteria yields the following expression for the collective pitch for neutral stability.

$$(\theta - A)^2 = \frac{P^2}{2(P-1)(2-P)} \times \left\{D + \frac{(D + A\theta)(P - W)^2}{\eta^2[W + P(D + A\theta)][1 + D + A\theta]} + \frac{2\beta_{pc}(P-1)}{\eta P^2}\left[\frac{2\beta_{pc}(P-1)}{\eta} - (3P - 4)(\theta - A)\right]\right\} \qquad (16)$$

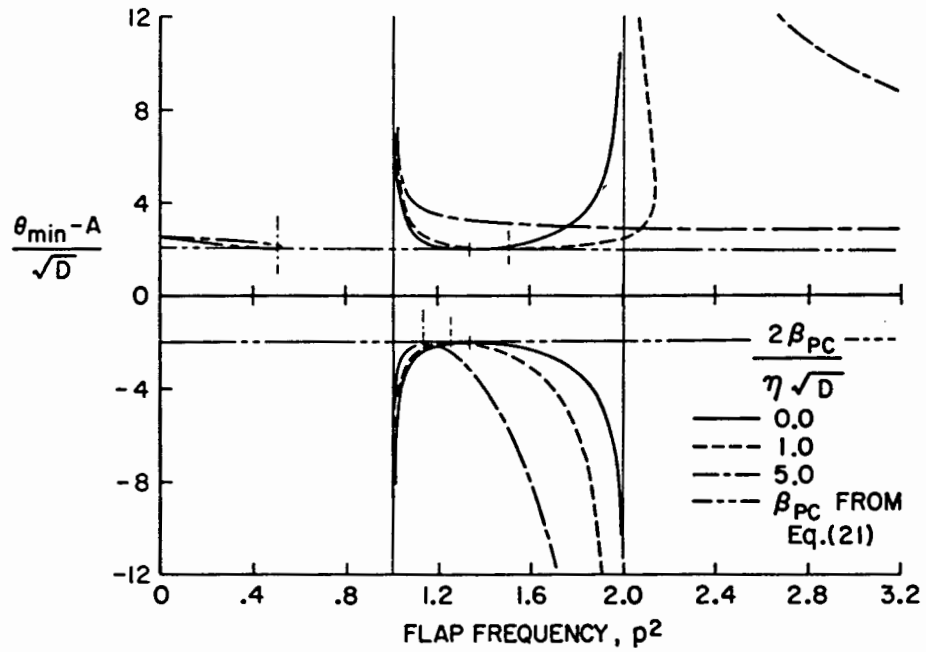

FIGURE 5. Effect of pre-cone on the minimum pitch angle for neutral stability, $\bar{\omega}_\zeta = p$.

We will first examine the case of "ideal" pre-cone, when the aerodynamic and inertial flap moments are exactly balanced and the hinge spring supplies zero flap moment.

$$\beta_{pc_i} = [\gamma/8](\theta - A) \tag{17}$$

Substitution into Eq. (16) indicates that instability is not possible. This is because the destabilizing flap-lag coupling is exactly cancelled by the lead-lag induced drag damping ($A\theta$ in Eq. 14). This indicates that pre-cone can be strongly stabilizing although further examination of Eq. (16) indicates that for $\beta_{pc} \neq \beta_{pc_i}$ pre-cone may also be destabilizing. The worst condition occurs when

$$\beta_{pc_w} = \frac{\eta}{4}\frac{(3P-4)}{(P-1)}(\theta - A) \tag{18}$$

The corresponding pitch angle for neutral stability is

$$(\theta - A)^2 = 4\left\{D + \frac{[D + A\theta][P - W]^2}{\eta^2[W + P(D + A\theta)][1 + D + A\theta]}\right\} \tag{19}$$

For a given flap frequency p, the least stable condition again occurs when $\bar{\omega}_\zeta = p$ but unlike basic flap-lag stability, it is independent of p. In other words $\theta_{min} = \theta^*$; Eq. (19) becomes for $a = 2\pi$

$$(\theta_{min} - A) = 2\sqrt{c_{d_0}/\pi} \tag{20}$$

The required pre-cone for least stability then becomes

$$\beta_{pc_w} = [\gamma/16][(3P-4)/(P-1)]\sqrt{c_{d_0}/\pi} \tag{21}$$

These results are illustrated in Fig. 5 by a plot of the normalized value of the minimum pitch angle for neutral stability, $(\theta_{min} - A)/\sqrt{D}$, as a function of the flap frequency, p. For simplicity $\bar{\omega}_\zeta = p$. For zero pre-cone the previous result for θ_{min} applies and $\theta_{min} = \theta^*$ when $p = \sqrt{4/3}$. For pre-cone variation with p according to Eq. (21) the absolute minimum θ^* occurs for any value of p. Even the previous limits $1 < p^2 < 2$ no longer apply. Also shown in Fig. 5 are stability boundaries for constant β_{pc} values. Minimum stability still occurs when $\bar{\omega}_\zeta = p$ although the positive and negative roots for θ_{min} are no longer equal. Furthermore, a sign change for β_{pc} or θ is equivalent. The general effect of pre-cone is to shift the flap frequency for least stability ($\theta_{min} = \theta^*$) away from $p = \sqrt{4/3}$. Indeed, θ^* occurs when p is given by Eq. (21). These results clearly show that pre-cone can be a destabilizing factor for flap-lag oscillations.

It may be noted that the above conclusions differ somewhat from previous results. In Ref. 2, it was concluded that for centrally hinged rigid blades in hover, destabilizing flap-lag coupling would vanish when flapping restraint vanished ($p = 1$, articulated blade) or when the blades were ideally pre-coned. As a result, flap-lag instabilities were precluded. The present study indicates that flap-lag coupling does not vanish under these conditions, for instance Eq. (5) indicates that $F_\zeta C_{\dot{\beta}} \neq 0$ for $p = 1$. This discrepancy can be attributed to the derivation of the aerodynamic flap and lead moments and is further discussed in the Appendix.

Case III, Variable Elastic Coupling

The applicable homogeneous equations for this case, taken from the Appendix are

$$\begin{bmatrix} s^2 + F_{\dot\beta}s + F_\beta & -sF_{\dot\zeta} + F_\zeta \\ -sC_{\dot\beta} + C_\beta & s^2 + C_{\dot\zeta}s + C_\zeta \end{bmatrix} \begin{Bmatrix} \Delta\beta \\ \Delta\zeta \end{Bmatrix} = 0 \quad (22)$$

The elastic coupling terms F_ζ and C_β produce cross coupled flap and lead-lag moments proportional to lead-lag and flap deflections respectively. Previous studies have typically neglected these terms in simplified rotor blade stability analyses. However, as will be seen below, they can have pronounced effects on the stability and dynamic characteristics of rotor blade flap-lag motion. For small pitch angles F_ζ and C_β are given by

$$R(\bar\omega_\zeta^2 - \bar\omega_\beta^2)\theta \quad (23)$$

Elastic coupling is proportional to pitch angle and is configuration dependent by virtue of the nonrotating lead-lag and flap frequencies $\bar\omega_\zeta$, $\bar\omega_\beta$, and the variable elastic coupling parameter R.

The elastic coupling of actual hingeless rotor blades is dependent on the particular design configuration and specifically the distribution of flexibility radially inboard and outboard of the pitch bearing. As explained in the Appendix, this characteristic is introduced in the rigid blade equations by dividing the flap and lead-lag hinge springs into two separate spring systems, one inboard and the other outboard of the pitch axis. The degree of elastic coupling is denoted by R and is proportional to the fraction of flexibility present in the spring system outboard of the hinge axis.

Representative results for the locus of roots of the lead-lag mode are shown in Fig. 6. In comparison with Fig. 2 it is apparent that the degree of elastic coupling R is highly important in determining whether the effects are stabilizing or destabilizing. For full elastic coupling, $R = 1.0$, the effect is generally highly stabilizing for the range of lead-lag frequencies considered. It is suggested that the elastic coupling allows the transfer of kinetic energy from the weakly damped inplane degree of freedom to the well damped flapping mode. As a result, the inherently low aerodynamic and structural lead-lag damping can easily be augmented by more than an order of magnitude. This is significant since it implies that the inplane degree of freedom is not as susceptible to instabilities as its low inherent damping would suggest.

Further examination of Fig. 6 indicates that small amounts of elastic coupling can be destabilizing for stiff inplane ($\bar\omega_\zeta > 1$) hingless rotors whereas soft inplane

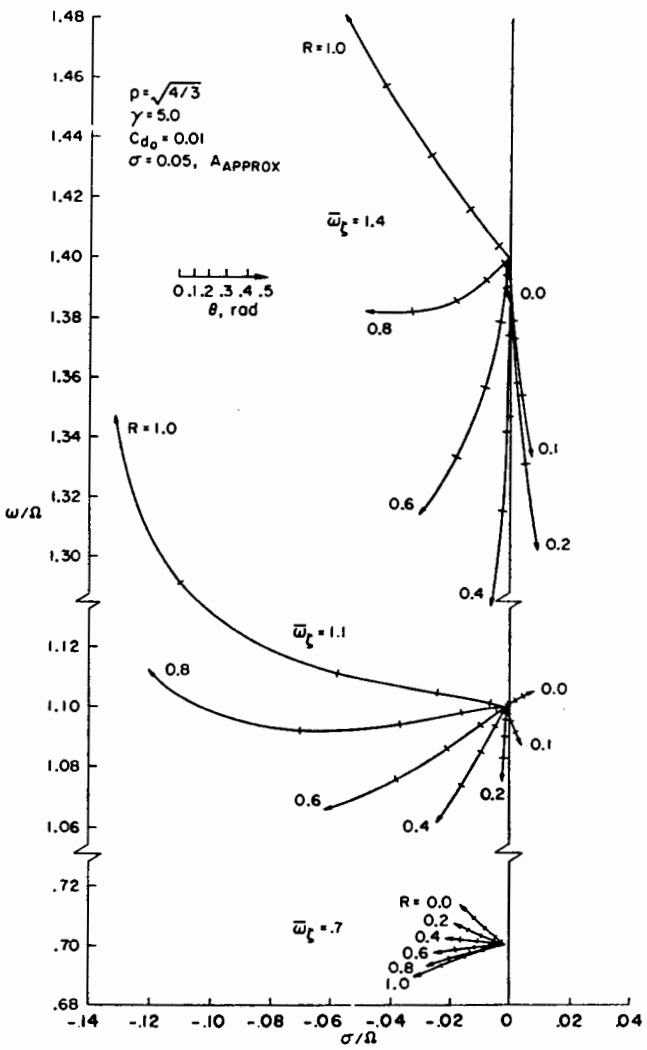

FIGURE 6. Locus of lead-lag mode roots, Case III, rigid blade equations with variable elastic coupling.

($\bar\omega_\zeta < 1$) rotor blades are only stabilized by elastic coupling. Further evidence is provided by Fig. 7 which presents stability boundaries for variable elastic coupling as a function of inplane frequency with $p = \sqrt{4/3}$. This figure clearly shows that for stiff inplane blades there exists a particular value of R for which instability can occur at moderately low pitch angles but that increased elastic coupling is strongly stabilizing. Furthermore, this minimum pitch angle is equal to θ^* given by Eq. (13) for the basic flap-lag equations.

Routh's criteria can be used to clarify these results. The equations with elastic coupling yield the following expression for the collective pitch for neutral stability.

$$(\theta - A)^2 = \frac{P^2}{2(P-1)(2-P)} \times \left\{ D + \frac{(D + A\theta)(W - P)^2 - Z(\theta + A)(W - P)[1 - (D + A\theta)] + Z^2[(D + A\theta + 1)^2 - (\theta + A)^2]}{\eta^2(D + A\theta + 1)[W + P(D + A\theta) + Z(\theta + A)]} \right\} \quad (24)$$

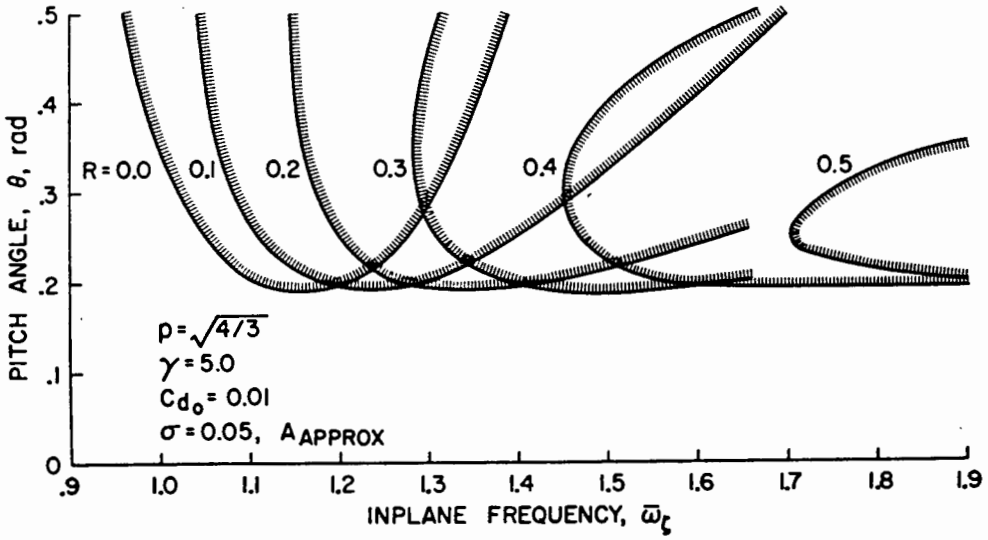

FIGURE 7. Stability boundaries for rigid blade equations with variable elastic coupling.

where

$$P = p^2,\ W = q^2,\ Z = z^2 \tag{25}$$

This expression neglects the effect of elastic coupling on β_0 which is consistent with dropping second order terms in the perturbation analysis. Equation (24) confirms that elastic coupling, Z, can be destabilizing; however, it can be shown that θ cannot be less than θ^*. For small pitch angles ($\theta^2 \ll 1$) Eq. (24) can be greatly simplified yielding

$$(\theta - A)^2 = \frac{P^2}{2(P-1)(2-P)} \times \left\{ D + \frac{\left[D - \frac{(\theta - A)^2}{4}\right](W-P)^2 + \left[\frac{(\theta + A)(W-P)}{2} - R\theta(W - P + 1)\right]^2}{\eta^2 W} \right\} \tag{26}$$

where now

$$P = \bar{\omega}_\beta^2 + 1,\ W = \bar{\omega}_\zeta^2 \tag{27}$$

This equation illustrates that for the elastic coupling to be destabilizing the lead-lag frequency must be such that $W > P$ or $W < P - 1$. This confirms the results of Fig. 6 that elastic coupling can be destabilizing for stiff inplane but not soft inplane rotor blades. Furthermore, when $p = \sqrt{4/3}$ the value of R corresponding to the least stable value of lead-lag frequency can be found since $(\theta^* - A)^2 = 4D$. Equation (26) then yields

$$R = \frac{\theta^* + A}{2\theta^*}\frac{(W - 4/3)}{(W - 1/3)} \tag{28}$$

The significance of this result is that when $p = \sqrt{4/3}$, it is not necessary that $\bar{\omega}_\zeta = p$ for neutral stability to occur at $\theta = \theta^*$ as is the case without elastic coupling. In other words, rotor blade configurations with inplane frequencies differing from p are subject to the same critical stability condition if the elastic coupling is in accord with Eq. (28).

Case IV, Pitch-lag Coupling

To provide further information about hingeless rotor blade stability characteristics, a brief examination of the influence of kinematic pitch-lag coupling has been made. Since the important torsional degree of freedom is not included in the present paper, this represents a restricted but convenient way of assessing the effects of pitching motion in comparison with flap-lag and elastic coupling effects. The previous equations with elastic coupling (Case III) together with the non-homogeneous pitch angle terms given in Eq. (50) were combined using the following pitch-lag relation.

$$\Delta\theta = \theta_\zeta \Delta\zeta \tag{29}$$

Representative results for stability boundaries with respect to collective pitch are given in Fig. 8 for both stiff and soft inplane rotor blade configurations. For the soft inplane configuration, pitch-lag instability can occur only for positive values of θ_ζ. Also, the effects of elastic coupling are relatively small, in fact slightly destabilizing. The results are entirely different for the stiff inplane configuration however, where elastic coupling plays a major role. First, for $R = 0.0$, negative values of θ_ζ are destabilizing in opposition to the soft

inplane result. Second, elastic coupling is strongly stabilizing for negative θ_ζ but becomes progressively destabilizing as R increases and θ_ζ becomes positive. As a result, it appears that elastic coupling is wholly as effective as pitch-lag coupling in determining the flap-lag stability of stiff inplane rotor blades. This implies that proper combinations of these two parameters might be used to improve, or "optimize" the stability characteristics of stiff inplane configurations.

MULTI-MODE ELASTIC BLADE EQUATIONS

The basic partial differential equations for a uniform untwisted rotating beam are presented in the Appendix, together with a brief outline of the method of solution. Particular care was required to insure that centrifugal and Coriolis forces which produce the destabilizing flap-lag coupling were retained in the derivation. These forces arise from blade radial displacements and tension variations resulting from perturbation deflections and velocities respectively. These effects are normally not included in elastic rotor blade equations. In addition, they do not have direct counterparts in the approximate rigid blade equations since radial displacements and tension do not appear explicitly in those equations.

Results obtained using the elastic blade modal equations are presented in Fig. 9. The first inplane mode damping is relatively high as a result of the elastic coupling. Because the principle elastic axes of the rotor blade rotate through the pitch angle θ for the entire length of the blade, the elastic coupling is equivalent to $R = 1.0$ for the rigid blade. The effect of number of the modes retained in the equations is relatively slight as far as the first inplane mode damping is concerned. A single flap and lead-lag mode are denoted by $n = 1$, two of each mode are included for $n = 2$. To illustrate the importance of the proper derivation of the elastic equations, the damping is also shown with the radial displacement and tension perturbations neglected. This gives a very unconservative result since the destabilizing flap-lag terms are not present.

A comparison with the rigid blade damping ($R = 1.0$) shows the approximate equations to be quite accurate. That this is a result of proper inclusion of elastic coupling is shown by the rigid blade result without elastic coupling ($R = 0.0$).

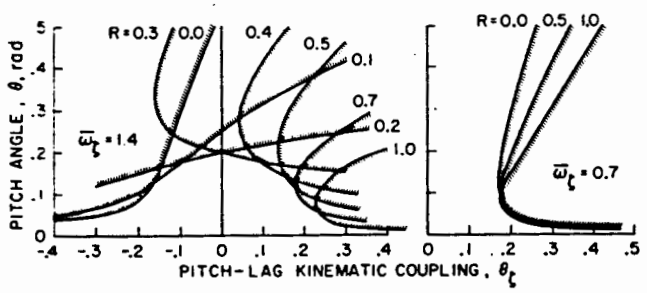

FIGURE 8. Stability boundaries for rigid blade equations, Case IV. kinematic pitch-lag coupling and variable elastic coupling, $p = \sqrt{4/3}$, $\gamma = 5.0$, $c_{d_0} = 0.01$, $\sigma = 0.05$.

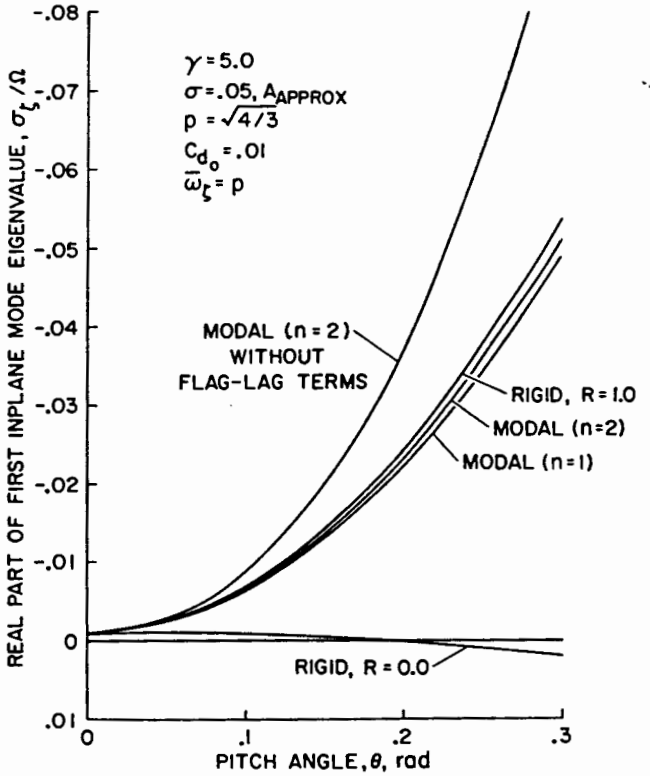

FIGURE 9. Comparison of inplane mode damping from approximate rigid blade equations and elastic blade modal equations.

EFFECT OF ELASTIC COUPLING ON FLAPPING RESPONSE

In addition to modifying the flap-lag stability characteristics, elastic coupling also produces significant variations in flapping frequency as collective pitch is increased. For a hingeless rotor blade this results in a variation in the phase lag of the blade flapping response to harmonic pitch excitations. The control inputs to a rotor from the swashplate are harmonic once-per-rev pitch changes and the flapping phase lag directly determines the ratio of the resulting rotor pitch and roll moments. The implications of elastic coupling can thus be appreciated in terms of vehicle stability and control characteristics.

The magnitude of the frequency shift is shown in Fig. 10 for the rigid blade with full elastic coupling and with aerodynamics neglected. At zero pitch the flap and lead-lag modes are uncoupled, but for $\theta = 0.3$ rad significant coupling exists. Note that elastic coupling vanishes when $\bar{\omega}_\beta = \bar{\omega}_\zeta$ and the frequencies are identical for all pitch angles.

Figure 11 illustrates the flapping response phase lar from pitch excitation for cases with and without elasti coupling. In particular, for stiff inplane rotor blades the influence of elastic coupling can be quite significant.

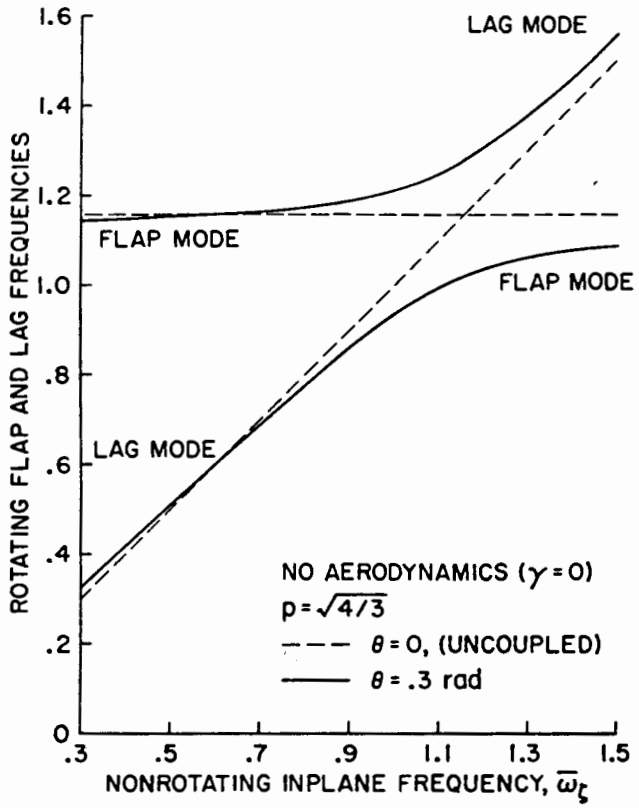

FIGURE 10. Effect of elastic coupling on rigid hinged blade flap and lead-lag frequencies without aerodynamics, R = 1.0.

Figure 12 further illustrates this effect as a function of collective pitch for a specific configuration.

CONCLUSIONS

The most important findings of the present study may be summarized as follows:

1) For torsionally rigid, spring restrained centrally hinged rotor blades flap-lag instability cannot occur in hover for pitch angles less than $\theta = \theta^*$.

2) Without pre-cone or elastic coupling, instability will not occur for practical pitch angles unless the inplane and flapping frequencies are reasonably close. For $\bar{\omega}_\zeta = p = \sqrt{4/3}$, neutral stability occurs at $\theta = \theta^*$.

3) Without elastic coupling the effect of pre-cone on stability may be either beneficial or detrimental. Ideal pre-cone eliminates flap-lag instability in hover.

4) Full elastic coupling virtually eliminates flap-lag instability and greatly augments the inherently low aerodynamic and structural damping of the lead-lag degree of freedom. Partial elastic coupling can be strongly destabilizing for stiff inplane rotor blades, however, and for $p = \sqrt{4/3}$ instability can occur for $\theta = \theta^*$ for a particular value of R.

5) The effects of kinematic pitch-lag coupling on flap-lag stability are highly dependent on elastic coupling for stiff inplane rotor blades, but not for soft inplane ones.

6) The flapping response phase for $1P$ pitch excitation is significantly altered by elastic coupling. This implies that coupled rotor-fuselage dynamic equations should include the rotor blade inplane degree of freedom.

7) The rigid hinged blade gives a reasonably accurate approximation of the actual elastic blade stability if the elastic coupling effects are properly accounted for.

APPENDIX

A brief derivation of the aerodynamic forces and equations of motion for both the rigid hinged blade and the elastic blade are given below. The basic x, y, z rotating coordinate system in Fig. 13 shows the positive conventions for angular (β,ζ) and linear (u,v,w) displacements (except a negative u displacement is shown).

AERODYNAMIC FORCES

The y and z components of the aerodynamic loading (lb/ft) can be written as follows

$$dF_z = dL - \phi dD \qquad dF_y = -dD - \phi dL \quad (30)$$

The elemental lift and drag forces can be written from simple strip theory. Since $\alpha = \theta - \phi$ and $\phi \simeq U_P/U_T$ for small inflow angles

$$dL = \frac{\rho a c}{2} V^2 \left(\theta - \frac{U_P}{U_T}\right) dx \qquad dD = \frac{\rho c V^2}{2} c_{d_0} dx \quad (31)$$

Combining Eqs. (30 and 31) and noting that $(U_P/U_T)^2 \ll 1$ yields

$$dF_z = \frac{\rho a c}{2} \left\{\theta U_T^2 - \left(1 + \frac{c_{d_0}}{a}\right) U_P U_T\right\} dx \quad (32)$$

$$dF_y = -\frac{\rho a c}{2} \left\{\frac{c_{d_0}}{a} U_T^2 + \theta U_P U_T - U_P^2\right\} dx \quad (33)$$

Incorporating the airfoil flap and lead displacements (v,w) in the rotating coordinate system, the relative fluid velocities become

$$U_P = v_i + \dot{w} \qquad U_T = \Omega x + \dot{v} \quad (34)$$

The final equations are then obtained after discarding second order products of displacement velocities $(\dot{w}^2,\dot{v}^2,\dot{w}\dot{v})$.

$$dF_z = \frac{\rho a c}{2} \left\{\theta \Omega^2 x^2 - \left(1 + \frac{c_{d_0}}{a}\right) \Omega x v_i + \dot{v}\left[2\Omega x\theta - v_i\left(1 + \frac{c_{d_0}}{a}\right)\right] - \Omega x \dot{w}\left(1 + \frac{c_{d_0}}{a}\right)\right\} dx \quad (35)$$

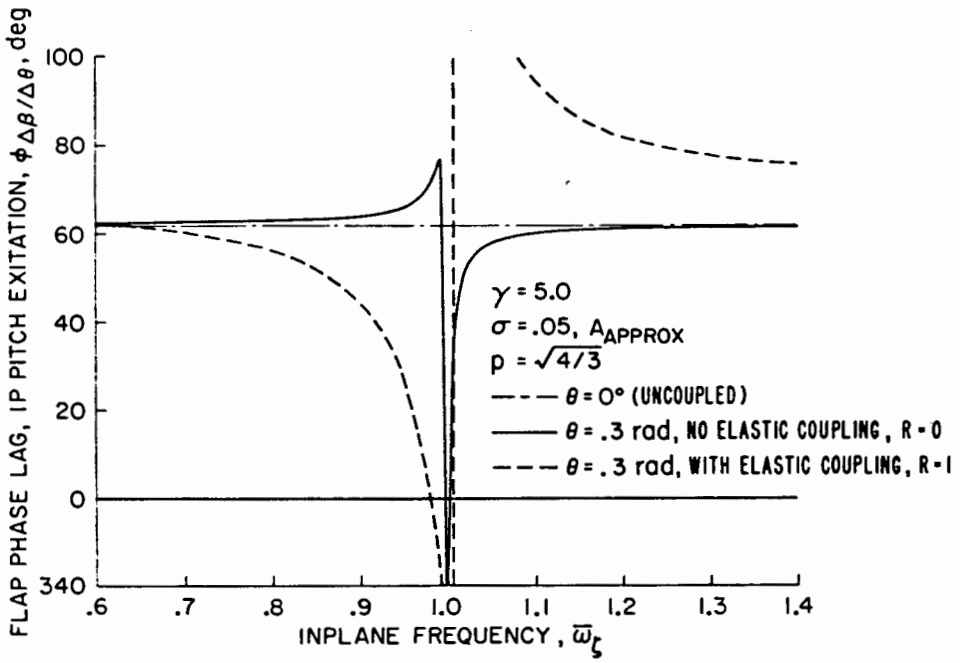

FIGURE 11. Effect of elastic coupling on flap response phase lag from pitch angle excitation, rigid blade.

$$dF_v = -\frac{\rho a c}{2}\left\{x^2\Omega^2\frac{c_{d_0}}{a} + \theta x\Omega v_t - v_t^2 + \dot{v}\left(2x\Omega\frac{c_{d_0}}{a} + \theta v_t\right) + \dot{w}(\theta\Omega x - 2v_t)\right\}dx \quad (36)$$

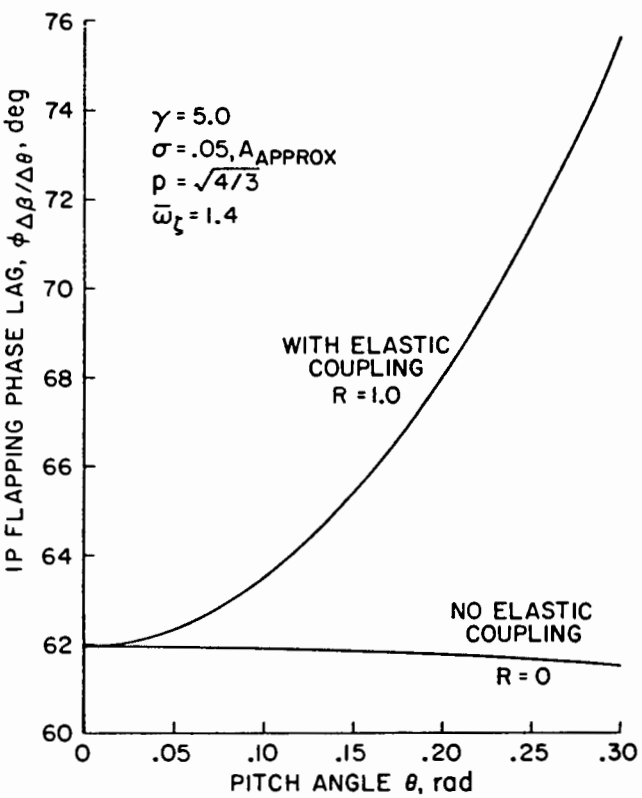

FIGURE 12. Flap response phase lag variation with collective pitch, rigid blade.

These are the general aerodynamic loading expressions including the effects of flap and lead velocities. The difference between the present results and those of Ref. 2 noted earlier lies in derivation of these equations. In Ref. 2, U_T in Eq. (31) was approximated by Ωx rather than the complete equation given by (34), $\Omega x + \dot{v}$. This results in an error in the coefficient of the first order $\dot{v}$ term in Eqs. (35) and (36).

For the elastic blades the aerodynamic loading can be applied directly to the relevant partial differential equations given below. For centrally hinged rigid blades, the aerodynamic moments about the hinges for the flap and lead-lag equations are easily developed. The kinematics of a rigid blade implies

$$v = x\dot{\zeta} \qquad w = x\dot{\beta} \quad (37)$$

The flap and lead aerodynamic moments are defined by

$$M_{\beta_{aero}} = \int_0^R x dF_z \qquad M_{\zeta_{aero}} = \int_0^R x dF_y \quad (38)$$

The resulting moments become, for constant chord,

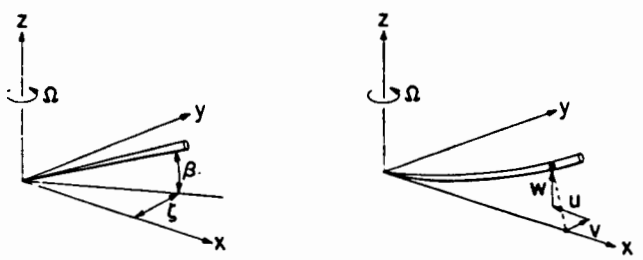

FIGURE 13. Rotor blade angular and rectilinear displacements in roating coordinate system.

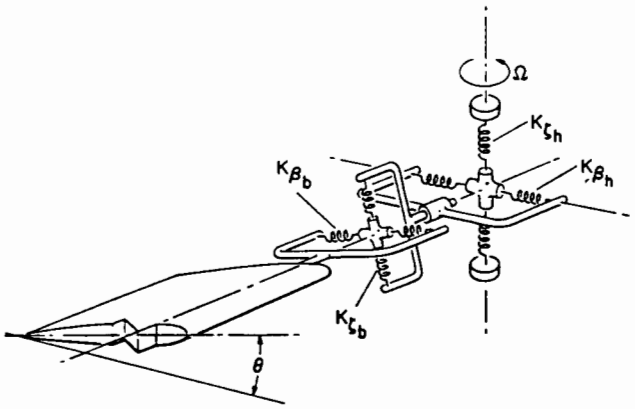

FIGURE 14. Arrangement of flap and lead-lag springs of rotor blade and hub for simulating variable elastic coupling. For clarity, rotor blade springs shown radially displaced from axis of rotation.

untwisted blades

$$M_{\beta_{aero}} = \frac{\gamma I\Omega^2}{8}\left\{\theta - \left(1 + \frac{c_{d_0}}{a}\right)A + \left[2\theta - \left(1 + \frac{c_{d_0}}{a}\right)A\right]\frac{\dot{\zeta}}{\Omega} - \left(1 + \frac{c_{d_0}}{a}\right)\frac{\dot{\beta}}{\Omega}\right\} \quad (39)$$

$$M_{\zeta_{aero}} = -\frac{\gamma I\Omega^2}{8}\left\{\frac{c_{d_0}}{a} + A\theta - C + \frac{\dot{\zeta}}{\Omega}\left(2\frac{c_{d_0}}{a} + A\theta\right) + \frac{\dot{\beta}}{\Omega}(\theta - 2A)\right\} \quad (40)$$

The integrals A, C and Lock number γ are defined by

$$A \equiv 4\int_0^1 \xi^2\left(\frac{v_t}{R\Omega}\right)d\xi,$$

$$C \equiv 4\int_0^1 \xi\left(\frac{v_t}{R\Omega}\right)^2 d\xi, \quad \gamma = \frac{\rho acR^4}{I} \quad (41)$$

Rigid Blade Equations

The inertial and elastic restraint moments about the centrally located flap and lead-lag hinges are combined with the aerodynamic moments to yield the equations of motion for a rigid hinged rotor blade. The inertial terms, including centrifugal and Coriolis moments are

$$M_{\beta_i} = -I(\ddot{\beta} + \Omega^2\beta + 2\Omega\beta\dot{\zeta}) \quad M_{\zeta_i} = -I(\ddot{\zeta} - 2\Omega\beta\dot{\beta}) \quad (42)$$

The elastic restraint hinge moment equations are developed for the spring configuration shown in Fig. 14. Two orthogonal spring systems are attached to the hub and blade inboard and outboard of the pitch axis respectively. The blade spring system, which rotates during collective pitch changes produces a significant cross coupling of flapping moments with lead-lag deflections and vice-versa. This effect, herein termed elastic coupling, is approximately proportional to the flexibility of the blade spring system relative to the total spring flexibility. Previous studies have treated only the uncoupled configuration, where all flexibility is contained in the hub spring system.

The configuration of Fig. 14 reduces to a simple equivalent single spring system at zero pitch angle which defines the rotor blade nonrotating frequencies. The equivalent spring system is given by

$$K_\beta = \frac{K_{\beta_B}K_{\beta_H}}{K_{\beta_B} + K_{\beta_H}}, \quad K_\zeta = \frac{K_{\zeta_B}K_{\zeta_H}}{K_{\zeta_B} + K_{\zeta_H}} \quad (43)$$

The complete elastic moments can be written as

$$M_{\beta_{elastic}} = -\frac{\beta}{\Delta}[K_\beta + R(K_\zeta - K_\beta\sin^2\theta] - \frac{\zeta R}{2\Delta}(K_\zeta - K_\beta)\sin 2\theta \quad (44)$$

$$M_{\zeta_{elastic}} = -\frac{\zeta}{\Delta}[K_\zeta - R(K_\zeta - K_\beta)\sin^2\theta] - \frac{\beta R}{2\Delta}(K_\zeta - K_\beta)\sin 2\theta \quad (45)$$

where

$$\Delta = 1 + R(1 - R)\frac{(K_\zeta - K_\beta)^2}{K_\zeta K_\beta}\sin^2\theta \quad (46)$$

The degree of elastic coupling is governed by R which is defined as

$$R = K_\beta/K_{\beta_B} = K_\zeta/K_{\zeta_B}$$
$$(1 - R) = K_\beta/K_{\beta_H} = K_\zeta/K_{\zeta_H} \quad (47)$$

Where $R = 0.0$ no elastic coupling is present and the hinge spring system is entirely contained at the hub and does not rotate with pitch angle changes. The converse is true for full elastic coupling, $R = 1.0$. Variations in elastic coupling are accommodated by intermediate values of R.

The final flap-lag equations are obtained by combining the aerodynamic, inertial, and elastic contributions. The usual perturbation method of solution is desired wherein

$$\theta(t) = \theta_0 + \Delta\theta(t), \quad \beta(t) = \beta_0 + \Delta\beta(t), \quad \zeta(t) = \zeta_0 + \Delta\zeta(t) \quad (48)$$

The equilibrium equations become

$$\begin{bmatrix} p^2 & z^2 \\ z^2 & q^2 \end{bmatrix}\begin{Bmatrix}\beta_0 \\ \zeta_0\end{Bmatrix} = \gamma/8\begin{Bmatrix}\theta - A \\ -\left(\frac{c_{d_0}}{a} + A\theta - C\right)\end{Bmatrix} \quad (49)$$

The perturbation equations, which neglect second order nonlinear products such as $\Delta\dot{\beta}\Delta\beta$, $\Delta\beta\Delta\dot{\zeta}$, $\Delta\theta\Delta\dot{\beta}$, and

$\Delta\theta\Delta\zeta$ are Laplace transformed to yield

$$\begin{bmatrix} s^2 + \frac{\gamma}{8}s + p^2 & -s\left[\frac{\gamma}{8}(2\theta - A) - 2\beta_0\right] + z^2 \\ -s\left[2\beta_0 - \frac{\gamma}{8}(\theta - 2A)\right] + z^2 s^2 + s\frac{\gamma}{8}\left(2\frac{c_{d_0}}{a} + A\theta\right) + q^2 & \end{bmatrix} \begin{Bmatrix} \Delta\beta \\ \Delta\zeta \end{Bmatrix} = \Delta\theta$$

$$\left[\frac{\gamma}{8}\begin{Bmatrix}1\\-A\end{Bmatrix} - R\frac{(\bar{\omega}_\zeta^2 - \bar{\omega}_\beta^2)}{\Delta}\left\{R_w\left[\begin{bmatrix}\beta_0 - \frac{\gamma}{8}(\theta - A)\\ \frac{\gamma}{8}\left(\frac{c_{d_0}}{a} + A\theta - C\right)\end{bmatrix}\right] + \left[\beta_0\begin{bmatrix}\sin 2\theta\\ \cos 2\theta\end{bmatrix} + \zeta_0\begin{bmatrix}\cos 2\theta\\ -\sin 2\theta\end{bmatrix}\right\}\right] \tag{50}$$

where

$$R_w = (1 - R)\frac{\bar{\omega}_\zeta^4 + \bar{\omega}_\beta^4}{\bar{\omega}_\zeta^2\bar{\omega}_\beta^2}\sin 2\theta$$

$$p^2 = 1 + \frac{1}{\Delta}\left[\bar{\omega}_\beta^2 + R(\bar{\omega}_\zeta^2 - \bar{\omega}_\beta^2)\sin^2\theta\right]$$

$$q^2 = \frac{1}{\Delta}\left[\bar{\omega}_\zeta^2 - R(\bar{\omega}_\zeta^2 - \bar{\omega}_\beta^2)\sin^2\theta\right] \tag{51}$$

$$z^2 = \frac{R}{2\Delta}(\bar{\omega}_\zeta^2 - \bar{\omega}_\beta^2)\sin 2\theta$$

$$\bar{\omega}_\beta^2 = K_\beta/I\Omega^2,\ \bar{\omega}_\zeta^2 = K_\zeta/I\Omega^2$$

Note that for convenience θ_0 has been written as θ in the final equations.

Elastic Blade Equations

Only a brief outline of the equation derivation for an elastic rotor blade will be given. Although the effects of pre-cone for the elastic blade were not investigated, this parameter is included in the following equations for generality. The equations are restricted to untwisted blades with uniform mass and stiffness distributions. In the case of pre-cone, the X axis is rotated through the angle β_{pc} about the Y axis. The following equations are similar to those derived in Ref. 7 except that radial deflections and nonlinear strain have been retained. They are, in order, the radial, inplane, and flapping displacement equations together with the nonlinear strain relation.

$$-T' + m[\ddot{u} - 2\Omega\dot{v} - \Omega^2(x + u) + \Omega^2 w\beta_{pc}] = 0 \tag{52}$$

$$-(Tv')' + K_{vv}v'''' + K_{vw}w'''' + m[\ddot{v} - \Omega^2 v + 2\Omega(\dot{u} - \beta_{pc}\dot{w})] = \frac{dF_y}{dx} \tag{53}$$

$$-(Tw')' + K_{ww}w'''' + K_{wv}v'''' + m[\ddot{w} - \Omega^2\beta_{pc}(w\beta_{pc} - (x + u)) + 2\Omega\beta_{pc}\dot{v}] = \frac{dF_z}{dx} \tag{54}$$

$$T = EA(u' + {}^1/_2v'^2 + {}^1/_2w'^2) \tag{55}$$

where

$$K_{vv} = E(I_2\cos^2\theta + I_1\sin^2\theta) \tag{56}$$

$$K_{ww} = E(I_1\cos^2\theta + I_2\sin^2\theta) \tag{57}$$

$$K_{wv} = K_{vw} = E(I_2 - I_1)\sin\theta\cos\theta \tag{58}$$

The solution proceeds in a manner similar to the rigid blade case, where the displacements are assumed to consist of steady state and perturbation components, $u(x,t) = u_0(x) + \Delta u(x,t)$, and similarly for v, w, and T. The steady state equations then become

$$-T_0' + m\Omega^2 w_0\beta_{pc} - m\Omega^2(x + u_0) = 0 \tag{59}$$

$$-(T_0v_0')' + K_{vv}v_0'''' + K_{vw}w_0'''' - m\Omega^2 v_0 = \frac{dF_{y_0}}{dx} \tag{60}$$

$$-(T_0w_0')' + K_{ww}w_0'''' + K_{wv}v_0'''' - m\Omega^2\beta_{pc}[w_0\beta_{pc} - (x + u_0)] = \frac{dF_{z_0}}{dx} \tag{61}$$

For $\beta_{pc} = 0$, a linear solution for v_0 and w_0 is easily obtained by Galerkin's method after discarding second order terms ($u_0 \ll x$) in Eqs. (59) and (61). For the perturbation equations we have

$$-\Delta T' - m(2\Omega\Delta\dot{v} - \Omega^2\Delta w\beta_{pc}) = 0 \tag{62}$$

$$-(T_0v')' - (\Delta Tv_0')' + K_{vv}\Delta v'''' + K_{vw}\Delta w'''' + m[\Delta\ddot{v} - \Omega^2\Delta v + 2\Omega(\Delta\dot{u} - \beta_{pc}\Delta\dot{w})] = \frac{d\Delta F_y}{dx} \tag{63}$$

$$-(T_0\Delta w')' - (\Delta Tw_0')' + K_{ww}\Delta w'''' + K_{wv}\Delta v'''' + m[\Delta\ddot{w} + 2\Omega\beta_{pc}\Delta\dot{v}] = \frac{d\Delta F_z}{dx} \tag{64}$$

$$\Delta T = EA[\Delta u' + v_0'\Delta v' + w_0'\Delta w'] \tag{65}$$

Equations (63) and (64) are the inplane and flapping perturbation equations for an elastic rotor blade. Without the perturbation tension, ΔT, and radial displace-

ment. Δu, terms these equations are conventional. However, the ΔT and Δu terms give rise to the destabilizing flap-lag effects and must be retained. The additional equations (62) and (65) can be substituted into Eqs. (63) and (64) to yield two equations in two unknowns Δv, Δw which are then solved by Galerkin's method. The flap and lead-lag displacements are exexpressed in series form.

$$\Delta v(x,t) = \sum_{n=1}^{N} V_n(t)\phi_{v_n}(x) \tag{66}$$

$$\Delta w(x,t) = \sum_{n=1}^{N} W_n(t)\phi_{w_n}(x) \tag{67}$$

ACKNOWLEDGEMENT

The authors wish to acknowledge the assistance of D. A. Peters, Research Scientist, AMRDL, for certain derivations given in this paper.

REFERENCES

1. Young, M. I., "A Theory of Rotor Blade Motion Stability in Powered Flight", *J. American Helicopter Society*, Vol. 9, No. 3 July 1964.
2. Hohenemser, K. H. and Heaton, P. W. Jr., "Aeroelastic Instability of Torsionally Rigid Helicopter Blades," *J. American Helicopter Society*, 2 (12) April 1967.
3. Gaffey, T. M., *The Effect of Positive Pitch-Flap Coupling (Negative δ_3) on Rotor Blade Motion Stability and Flapping*, Proceedings, American Helicopter Society 24th Annual National Forum, Washington, D.C. May 1968.
4. Jenkins, J. L. Jr., *A Parametric Study of Blade Motion Stability Boundaries for an Articulated Rotor*, NASA TND-5032, February 1969.
5. Hall, W. E. Jr., *Application of Floquet Theory to the Analysis of Rotary-Wing VTOL Stability*, Stanford University, SUDAAR No. 400 February 1970.
6. Gessow, A. and Myers, G. D., Jr., *Aerodynamics of the Helicopter*, Frederick Ungar Publishing Company, New York, 1967.
7. Houbolt, J. C. and Brooks, G. W., *Differential Equations of Motion for Combined Flapwise Bending, Chordwise Bending, and Torsion of Twisted Nonuniform Rotor Blades*, NACA Report 1346, October 1956.

For $\Omega = 1$ $\quad (\Delta = 1)$

$$\gamma^2 = \omega_\zeta^2 c_\theta^2 + \omega_\beta^2 s_\theta^2$$

$$p^2 = 1 + \omega_\beta^2 c_\theta^2 + \omega_\zeta^2 s_\theta^2$$

$$\epsilon^2 = (\omega_\zeta^2 - \omega_\beta^2) s_\theta c_\theta$$